Application of the Ensemble Kalman Smoother to Turbulent Transport Analysis in LHD Plasma*)

Yuya MORISHITA, Sadayoshi MURAKAMI, Masayuki YOKOYAMA[1,3)] and Genta UENO[2,3,4)]

Department of Nuclear Engineering, Kyoto University, Kyoto 615-8540, Japan
[1)]*National Institute for Fusion Science, Toki 509-5292, Japan*
[2)]*The Institute of Statistical Mathematics, Tokyo 190-8562, Japan*
[3)]*The Graduate University for Advanced Studies, SOKENDAI, Toki 509-5292 and Tokyo 190-8562, Japan*
[4)]*The Joint Support-Center for Data Science Research, Tokyo 190-0014, Japan*

(Received 15 November 2020 / Accepted 21 December 2020)

The ensemble Kalman smoother (EnKS) is introduced to the data assimilation system, ASTI, based on the integrated transport simulation code, TASK3D. We use the EnKS to estimate state variables composed of electron and ion temperature, density, and numerical factors of turbulent transport models and neutral beam injection (NBI) heat deposition. The time series data of plasma temperature and density profiles are assimilated into TASK3D. The estimation performance of the EnKS is investigated, and the EnKS is applied to an NBI plasma in the Large Helical Device (LHD) (shot:114053) to estimate the factors of the turbulent heat transport model. The obtained factors can reproduce the experimental temperature data with high accuracy. These results indicate the effectiveness and validity of the EnKS approach for accurate estimation of fusion plasma parameters.

Keywords: data assimilation, ASTI, ensemble Kalman smoother, TASK3D, LHD

DOI: 10.1585/pfr.16.2403016

1. Introduction

Integrated simulation for fusion plasmas has various uncertainties in the employed simulation models, specifically, the turbulent transport model. Thus, the simulation results also have uncertainties and it is difficult to predict the behavior of fusion plasmas with high accuracy. Evaluating the employed simulation models while simultaneously considering more than one uncertainty in the simulation is difficult. To overcome this problem, we are developing a data assimilation system, ASTI [1].

In Ref. [1], a data assimilation technique, the ensemble Kalman filter (EnKF) [2] was introduced to an integrated transport simulation by TASK3D [3] for a plasma in the Large Helical Device (LHD). The electron and ion temperature profiles and temporal variations obtained by ASTI agreed well with measured values. In addition, ASTI has estimated the factors of turbulent heat transport models, which can reproduce experimentally measured temperature and density data. However, temporal variations of the filtered estimates are known to have a time delay from measured values because the EnKF optimizes the state vector using only past data (prior to the time of filtering) [4]. To estimate the state vector in a reasonable manner, not only spatially but also temporally, a data assimilation method that assimilates both past and future data is required.

In this study, the ensemble Kalman smoother (EnKS) [2], which corrects the filtered estimates by EnKF using future data (posterior to the time of filtering), is introduced to ASTI. We examine the performance of EnKS using simple examples, then apply EnKS to a typical high ion temperature neutral beam injection (NBI) plasma in the LHD (shot:114053) to estimate the factors of turbulent heat transport models.

Data assimilation methods can simultaneously estimate more than one parameter, or variable having its own uncertainty, and any variables connected with observed variables in a simulation model. Similar techniques based on Kalman filters have been applied for the safety factor profile estimation of tokamak plasmas [5]. The extended Kalman filter, which has been employed in Ref. [5], needs a linear approximation of the system model and does not always work well for nonlinear system models. The data assimilation method, which assimilates both past and future data, has not yet been implemented. On the other hand, EnKF and EnKS do not need the linear approximation and are strong, even for nonlinear system models.

This paper is organized as follows. Section 2 explains the data assimilation methods and the integrated simulation by TASK3D. Section 3 shows the settings of assimilation experiments and results of the data assimilation are described in Section 4. Finally, Section 5 presents a summary and conclusions.

author's e-mail: morishita.yuya.47r@st.kyoto-u.ac.jp

*) This article is based on the presentation at the 29th International Toki Conference on Plasma and Fusion Research (ITC29).

2. Methods

ASTI is a data assimilation system for toroidal fusion plasmas based on the EnKF and an integrated transport simulation code, TASK3D. In TASK3D, the one dimensional (1D) diffusive transport equation is solved for radial transport. In this study, only the following heat transport equations are solved for each electron and ion;

$$\begin{aligned}\frac{\partial}{\partial t}\left(\frac{3}{2}n_sT_sV^{5/3}\right)&=-V^{2/3}\frac{\partial}{\partial\rho}\left[V'\langle|\rho|\rangle n_sT_s\left(V_{K_s}+\frac{3}{2}V_s\right)\right.\\&\left.-V'\langle|\rho|^2\rangle\frac{3}{2}D_sT_s\frac{\partial n_s}{\partial\rho}-V'\langle|\rho|^2\rangle n_s\chi_s\frac{\partial T_s}{\partial\rho}\right]\\&+P_sV^{5/3},\end{aligned}\tag{1}$$

where ρ, n_s and T_s are the normalized minor radius, the density, and the temperature of the s-species, respectively. V is the plasma volume and $V' = \mathrm{d}V/\mathrm{d}\rho$. V_s is particle pinch velocity, V_{K_s} is the heat pinch velocity, and $\langle\rangle$ represents the magnetic flux surface average. D_s and χ_s are the particle and thermal diffusion coefficients, respectively. P_s is the power source, NBI heating and electron cyclotron heating (ECH), including the power exchange between the thermal particles and the fast neutrals. χ_s is assumed to be the sum of the neoclassical (NC) transport term and the turbulent (TB) transport term: $\chi_s = \chi_s^{\mathrm{NC}} + \chi_s^{\mathrm{TB}}$. In this paper, the gyro-Bohm model for the electron, as given in Eq. (2), and the gyro-Bohm grad$T$ model for the ion, as given in Eq. (3), are employed based on previous TASK3D simulations for LHD plasmas [6, 7]:

$$\chi_{\mathrm{e}}^{\mathrm{TB}} = C_{\mathrm{e}}\frac{T_{\mathrm{e}}}{eB}\frac{\rho_{\mathrm{i}}}{a},\tag{2}$$

$$\chi_{\mathrm{i}}^{\mathrm{TB}} = C_{\mathrm{i}}\frac{T_{\mathrm{i}}}{eB}\frac{\rho_{\mathrm{i}}}{a}\left(\frac{\nabla T_{\mathrm{i}}}{T_{\mathrm{i}}}a\right),\tag{3}$$

where B is the magnetic field strength, ρ_{i} is the ion Larmor radius, a is the plasma minor radius, and C_{e} and C_{i} are constant factors chosen based on experimental results [6]. The neoclassical transport coefficients, $\chi_{\mathrm{e}}^{\mathrm{NC}}$ and $\chi_{\mathrm{i}}^{\mathrm{NC}}$ are calculated by the DGN/LHD module [8] and the equilibrium magnetic field is calculated by VMEC code [9]. The NBI heat source $P_{\mathrm{NBI},s}$ is evaluated by the NBI heating analysis code, GNET-TD [10].

Data assimilation by EnKF and EnKS assumes a state-space model, which consists of a system model and an observation model, as given by Eqs. (4) and (5), respectively.

$$\mathbf{x}_t = f_t(\mathbf{x}_{t-1}, \mathbf{v}_t),\tag{4}$$

$$\mathbf{y}_t = H_t\mathbf{x}_t + \mathbf{w}_t.\tag{5}$$

The system model describes the temporal evolution of the state vector $\mathbf{x}$ from time $t-1$ to t with system noise $\mathbf{v}_t$. In the observation model, the state vector $\mathbf{x}_t$ is projected on the observation space by matrix H_t, and Gaussian observation noise $\mathbf{w}_t$ is added to the projected vector.

The EnKF procedure is a loop of prediction and filtering. In the prediction step, the predicted distribution of $\mathbf{x}_t$ given $\mathbf{y}_{1:t-1} \equiv \{\mathbf{y}_1, \cdots, \mathbf{y}_{t-1}\}$, $p(\mathbf{x}_t|\mathbf{y}_{1:t-1})$ is approximated by an ensemble consisting of

$$\mathbf{x}_{t|t-1}^{(n)} = f_t(\mathbf{x}_{t-1|t-1}^{(n)}, \mathbf{v}_t^{(n)}),\tag{6}$$

for the index of the ensemble members, $n = 1, \cdots, N$. It is noted that $\mathbf{x}_{t|s}^{(n)}$ is the n-th ensemble member that approximates the state distribution at time t given $\mathbf{y}_{1:s}$, $p(\mathbf{x}_t|\mathbf{y}_{1:s})$. Therefore, $\mathbf{x}_{t-1|t-1}^{(n)}$ is the n-th ensemble member that approximates the filtered state distribution at the previous time step, $p(\mathbf{x}_{t-1}|\mathbf{y}_{1:t-1})$. $\mathbf{v}_t^{(n)}$ is the n-th sample drawn from the distribution of system noise, $p(\mathbf{v}_t)$, and the Gaussian distribution is assumed as $p(\mathbf{v}_t)$ in this study. In ASTI, TASK3D is employed as the temporal evolution model f_t. In the filtering step, the current filtered estimate is obtained by Eq. (7) for each ensemble member.

$$\begin{aligned}\mathbf{x}_{t|t}^{(n)} &= \mathbf{x}_{t|t-1}^{(n)} + \hat{K}_t(\mathbf{y}_t - H_t\mathbf{x}_{t|t-1}^{(n)} + \mathbf{w}_t^{(n)}),\\ \hat{K}_t &= \hat{V}_{t|t-1}H_t^{\mathrm{T}}(H_t\hat{V}_{t|t-1}H_t^{\mathrm{T}} + R_t)^{-1}.\end{aligned}\tag{7}$$

Here, $\mathbf{w}_t^{(n)}$ is the n-th sample drawn from the distribution of observation noise $p(\mathbf{w}_t)$ and $\hat{V}_{t|t-1}$ is a sample covariance matrix of $\mathbf{x}_{t|t-1}^{(n)}$. R_t is the covariance matrix of the observation noise, that is, $\mathbf{w}_t \sim N(\mathbf{0}, R_t)$, where $N(\mathbf{0}, R_t)$ is the Gaussian distribution with zero mean and covariance matrix R_t. The superscript T denotes the matrix transposition.

The filter optimizes the state vector to enhance the prediction capability of the simulation model based on the observation data. The filtered estimate includes information that should be considered in the simulation model. However, it is known that there is a time difference between the filtered estimate and observation, because the filtered estimate is based on the observation data prior to the time of filtering. To estimate the state vector in a reasonable manner both temporally and spatially, the EnKS is more appropriate. The EnKS corrects the filtered estimate by the EnKF using observation data posterior to the time of filtering (future data).

The smoothing calculation by EnKS can be easily performed by storing a matrix that reconstructs the ensemble members at the filtering step. To derive the matrix representation of the filtering calculation, we introduce the following matrices,

$$\begin{aligned}X_{t|*} &= \left(\mathbf{x}_{t|*}^{(1)}, \mathbf{x}_{t|*}^{(2)}, \cdots \mathbf{x}_{t|*}^{(N)}\right),\\ \check{X}_{t|*} &= \left(\mathbf{x}_{t|*}^{(1)} - \hat{\mathbf{x}}_{t|*},\ \mathbf{x}_{t|*}^{(2)} - \hat{\mathbf{x}}_{t|*},\ \cdots, \mathbf{x}_{t|*}^{(N)} - \hat{\mathbf{x}}_{t|*}\right),\\ W_t &= \left(\mathbf{w}_t^{(1)}, \mathbf{w}_t^{(2)}, \cdots, \mathbf{w}_t^{(N)}\right),\\ Y_t &= (\mathbf{y}_t, \mathbf{y}_t, \cdots, \mathbf{y}_t),\end{aligned}$$

where $\hat{\mathbf{x}}_{t|*}$ is the sample mean of $\mathbf{x}_{t|*}^{(n)}$, and the matrix Y_t has N columns. Using these matrices, the filtering calculation given by Eq, (7) can be written as follows:

$$X_{t|t} = X_{t|t-1}Z_t,\tag{8}$$

$$\begin{aligned}Z_t = I + \check{X}_{t|t-1}^{\mathrm{T}}H_t^{\mathrm{T}}(H_t\hat{V}_{t|t-1}H_t^{\mathrm{T}} + R_t)^{-1}\\ \times (Y_t + W_t - H_tX_{t|t-1}),\end{aligned}\tag{9}$$

where I is an $N \times N$ identity matrix. The smoothed ensemble at time u using the observation data until time $u+1$, $X_{u|u+1}$, can be obtained by Eq. (10) using the filtered ensemble at time u, $X_{u|u}$, and the reconstruction matrix at time $u+1$, Z_{u+1} [2].

$$X_{u|u+1} = X_{u|u} Z_{u+1}. \tag{10}$$

Using Eq. (10), the recursion formula of the smoothed ensemble is written as

$$X_{u|t+1} = X_{u|t} Z_{t+1}, \tag{11}$$

where $t > u$. This means that the smoothed estimate at time u, based on the observation data up to an arbitrary time $t(> u)$, can be calculated as follows:

$$X_{u|t} = X_{u|u} Z_{u+1} Z_{u+2} \cdots Z_t. \tag{12}$$

This smoothing calculation can be executed only by storing the reconstruction matrix Z at every filtering step.

The smoothed ensemble matrices for time series data $\mathbf{y}_1, \mathbf{y}_2, \cdots, \mathbf{y}_T$ are calculated efficiently by the following procedure (fixed-interval smoother):

1. Determine the initial ensemble matrix $X_{0|0}$ and store this matrix.
2. Execute the EnKF until the time T storing the filtered ensemble matrix $X_{t|t}$ and the reconstruction matrix Z_t at every filtering step ($t = 1, 2, \cdots, T$).
3. Initialize a matrix A to a unit matrix and $t \leftarrow T-1$.
4. At time t, $A \leftarrow Z_{t+1} A$ and obtain the smoothed ensemble matrix at time t by $X_{t|T} = X_{t|t} A$.
5. Set $t \leftarrow t-1$ and repeat step 4, until all smoothed ensemble matrices are obtained.

In this paper, we estimate the factors of the turbulent heat transport models, which can reproduce a time series data-set of plasma temperature, using the EnKS. We consider the uncertainties of temperature T_s, density n_s, the constant factor in the turbulent transport models, C_s, and NBI heat deposition term $P_{\mathrm{NBI},s}$. The state vector is defined as follows:

$$\mathbf{x}_t = (\mathbf{T}_{\mathrm{e},t}^{\mathrm{T}}, \mathbf{T}_{\mathrm{i},t}^{\mathrm{T}}, \mathbf{n}_{\mathrm{e},t}^{\mathrm{T}}, \mathbf{n}_{\mathrm{i},t}^{\mathrm{T}}, \mathbf{C}_{\mathrm{e},t}^{\mathrm{T}}, \mathbf{C}_{\mathrm{i},t}^{\mathrm{T}}, \mathbf{k}_{\mathrm{e},t}^{\mathrm{T}}, \mathbf{k}_{\mathrm{i},t}^{\mathrm{T}})^{\mathrm{T}}. \tag{13}$$

Every state variable is defined on 60 computational grid points (radial direction, 1D) and has a similar structure as follows:

$$\mathbf{T}_{\mathrm{e}} = (T_{\mathrm{e}}^1, T_{\mathrm{e}}^2, \cdots, T_{\mathrm{e}}^{60})^{\mathrm{T}}. \tag{14}$$

The superscript on each element in Eq. (14) indicates the grid point. In Eq. (13), $\mathbf{T}, \mathbf{n}, \mathbf{C}$, and $\mathbf{k}$ denote the temperature, density, numerical factor of the turbulence models in Eqs. (2,3), and the factor for the NBI heat deposition, with i and e for ion and electron, respectively.

Table 1 The rates of the standard deviation of initial background error and system noise.

State variable	Initial background error	System noise
T_{e}	5%	10%
T_{i}	5%	10%
n_{e}	5%	10%
n_{i}	5%	10%
C_{e}	20%	20%
C_{i}	20%	20%
k_{e}	5%	5%
k_{i}	5%	5%

TASK3D can solve the time evolution of the particle density and the temperature. In this paper, TASK3D solves only the time evolution of the temperature, because the temporal variation of density is relatively small. The observation densities of the ion and electron have the same values, that is, $n_{\mathrm{e}} = n_{\mathrm{i}}$. The density is assumed to be stationary in the prediction step but is updated in the filtering step. Since factor C_s is assumed to be grid-dependent, as Eq. (14), C is allowed to have spatial variation. The factor k_{s}^i is defined to adjust the NBI heat deposition evaluated by GNET-TD. The following P_{s}^* is used instead of P_{s} in Eq. (1):

$$P_{\mathrm{s}}^{*i} = k_{\mathrm{s}}^i P_{\mathrm{s}}^i. \tag{15}$$

The initial ensemble mean is set to the observed data for T_s and n_s, and to the conventional values for C_s and k_s, that is, $C_{\mathrm{e}} = 23.0$, $C_{\mathrm{i}} = 9.07$ [6, 7], $k_{\mathrm{e}} = 1$, and $k_{\mathrm{i}} = 1$. The initial standard deviation of the ensemble and the system noise are set to be proportional to the ensemble mean, and their rates are listed in Table 1. The noise of k_s is assumed to be smaller than that of C_s. This means that the NBI heat deposition model (GENT-TD) is more reliable than the turbulent transport models. This assumption distinguishes the roles of k_s and C_s, and allows stable estimation of these terms. The standard deviation of observation noise is estimated before every filtering step to be proportional to the difference between the prediction and the observed data, whose rate is 0.8 [1].

3. Settings of Observation Data

For the assessment of the estimation by the EnKS, assimilation experiments are performed for four time series data-sets of temperature and density simulated by TASK3D (Cases 1 through 4). After the assimilation experiments, we apply the EnKS to an experimental data-set in the LHD (Case 5). The simulated observation data are generated by TASK3D for four different time-space distributions of factor C_{e} and C_{i}. The noise generated from the Gaussian distribution, whose mean is zero and standard deviation is 5% of the simulated value, is added to the simulated data as a measurement error. In all cases, the

NBI heat deposition precalculated by GNET-TD for shot 114053 is used.

In Case 1, C_e and C_i are constants and $C_s/C_{s0} = 1.5$, as shown in Fig. 1 (a), where C_{s0} denotes the conventional values of C_e and C_i ($C_e = 23.0$, $C_i = 9.07$). In Case 2, C_e and C_i have the temporal variation $C_s/C_{s0} = 1 + 0.5 \times \sin(2\pi t/1.0)$, as in Fig. 1 (b), where t is the time in seconds. This case corresponds to slow temporal variation compared with the cycle of assimilation $\tau_{DA} = 80$ ms. In Case 3, C_e and C_i have the temporal variation $C_s/C_{s0} = 1 + 0.25 \times \sin(2\pi t/0.1)$. This case corresponds to fast temporal variation compared with the cycle of assimilation $\tau_{DA} = 160$ ms. In Case 4, C_e and C_i have the spatial variation $C_s/C_{s0} = 1 + 0.5 \times \cos(2\pi\rho)$ as in Fig. 1 (c), where ρ is the normalized minor radius. In Case 5, we apply the EnKS to experimental data, an NBI plasma in the LHD (shot number:114053). To make the observed data easily

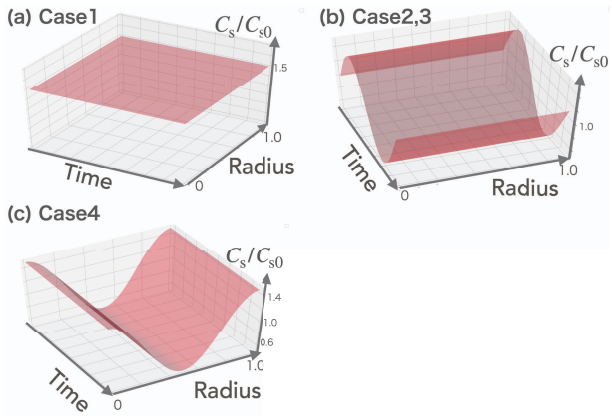

Fig. 1 Time-space distributions of C_e/C_{e0} and C_i/C_{i0} for Cases 1 through 4 in Table 2.

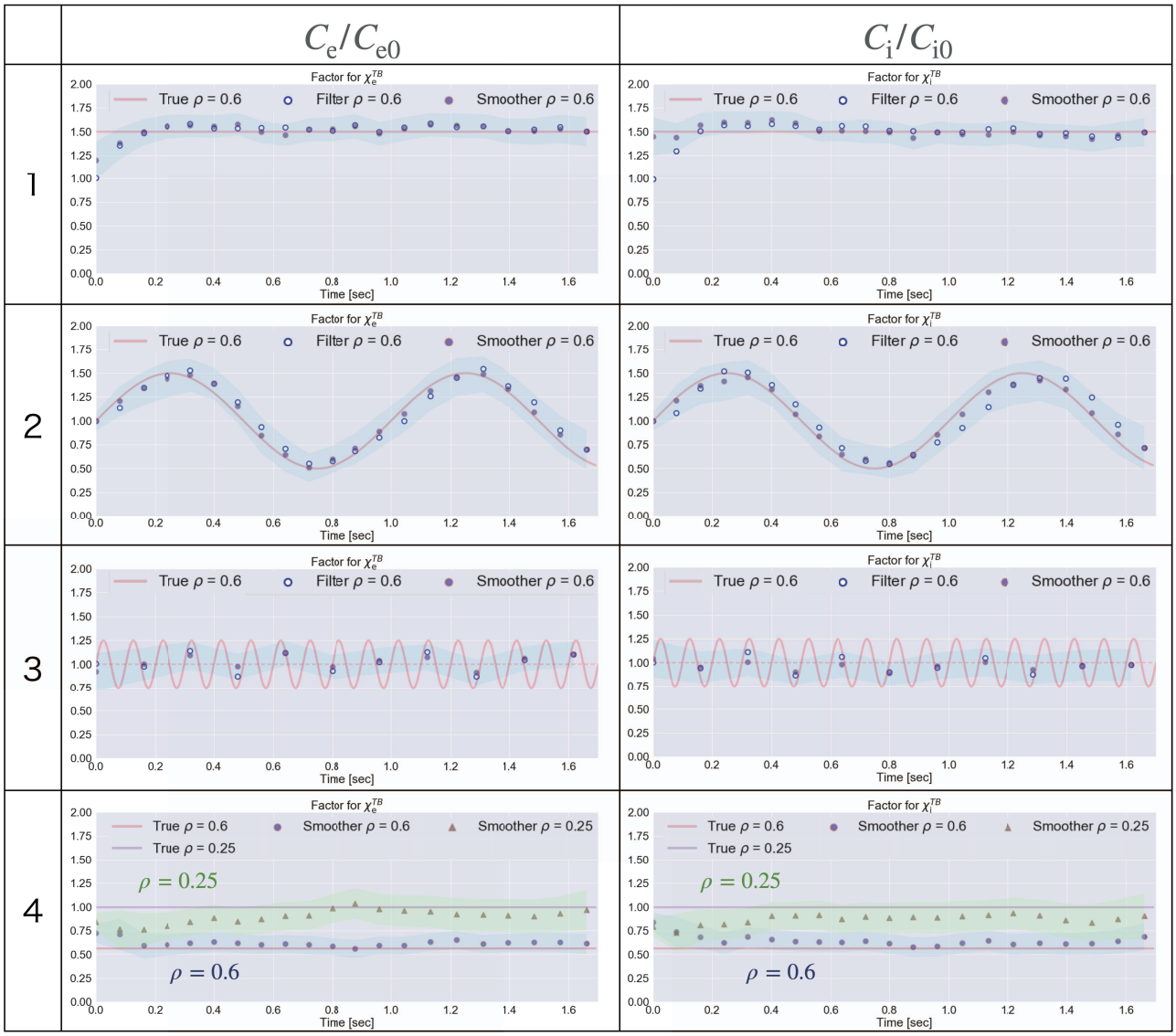

Fig. 2 Assimilation results of temporal change of C_e/C_{e0} and C_i/C_{i0} in Cases 1 through 4. The highlighted areas around the smoothed estimates represent the standard deviations of the smoothed ensemble.

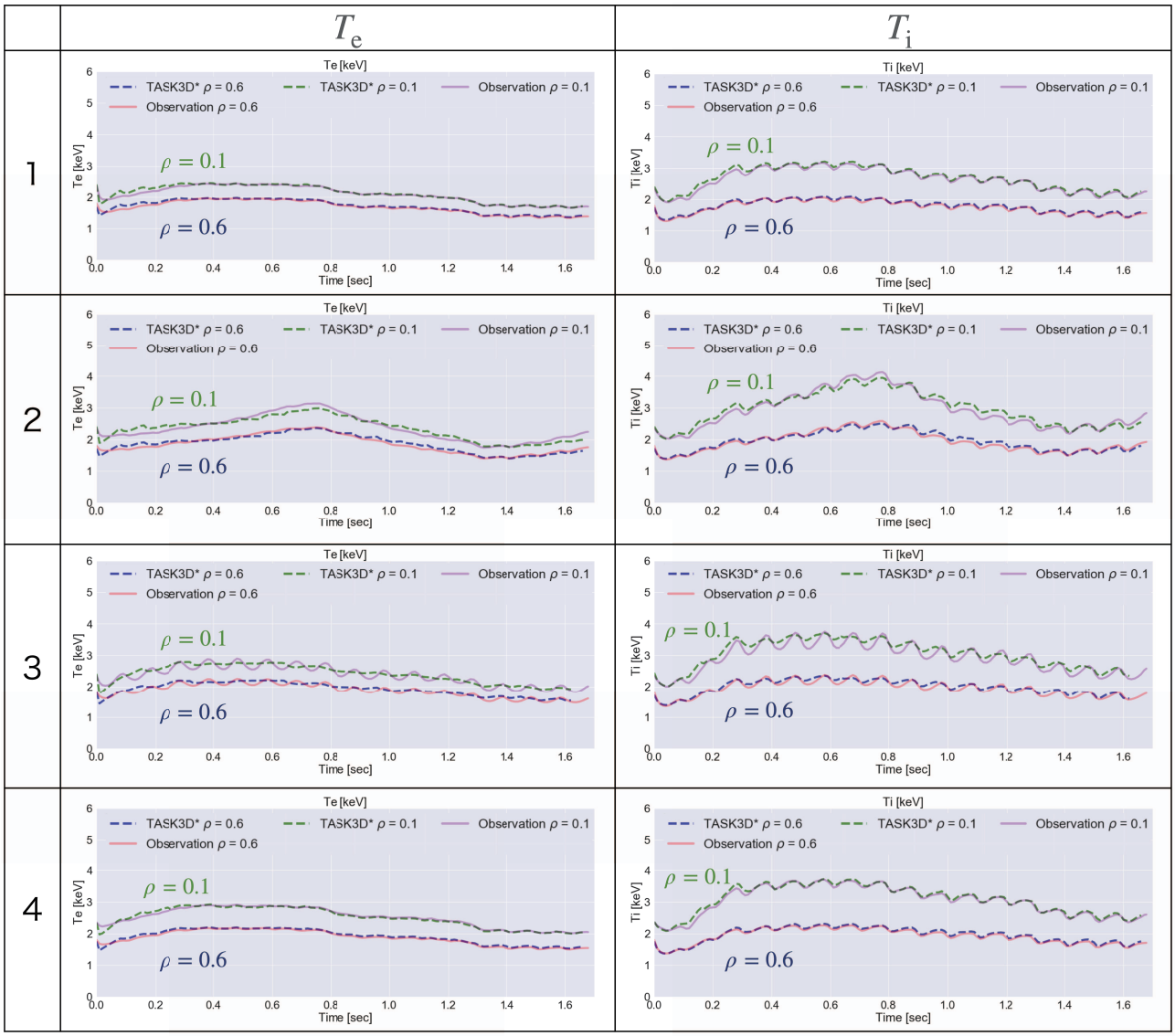

Fig. 3 TASK3D simulation results of T_e and T_i using the smoothed estimates of C_s and k_s for $\rho = 0.1$ and $\rho = 0.6$ in Cases 1 through 4.

assimilated, the temperature and density time series data are fit by a sixth order polynomial (only even degrees) in the radial direction and linearly interpolated in the time direction. Assimilation starts at 3.4 s in the shot and this time is set to 0.0 s in the simulation. Because the T_i observation data exist from 0.2 s, the T_e data are assimilated instead of T_i data, in the period from 0.0 s to 0.2 s. These assimilations are performed with 2000 ensemble members for $\tau_{DA} = 80$ ms (Cases 1, 2, 3, and 5) and $\tau_{DA} = 160$ ms (Case 4). A summary of these assimilations are shown in Table 2.

Table 2 Setup of data assimilation experiments.

Case	Observation data	True C_s/C_{s0}	τ_{DA}[ms]
1	Simulated data	constant : 1.5	80
2	Simulated data	$1 + 0.5 \times \sin(2\pi t/1.0)$	80
3	Simulated data	$1 + 0.25 \times \sin(2\pi t/0.1)$	160
4	Simulated data	$1 + 0.5 \times \cos(2\pi\rho)$	80
5	Experimental data		80

4. Assimilation Results

The temporal changes of filtered estimates and smoothed estimates of C_s/C_{s0} in Cases 1 to 4 are shown in Fig. 2. In Case 1, the filtered estimates approach the true values within the first few times of assimilation and stay around the true values. In this case, it is found that the EnKS estimates do not differ much form those of the EnKF, because the true values of C_e and C_i are stationary. In Case 2, it seems that the EnKF and EnKS can follow the slow temporal change of C_s, however, the estimates of EnKF have 0.04-0.08 s delays from the true values (for example, at $t = 0.96$, 1.04, and 1.12 in both C_e/C_{e0} and C_i/C_{i0}). The EnKS correcting the time delays, almost all the smoothed estimates are close to the true curve lines. In Case 3, the estimates, especially by the EnKS, are

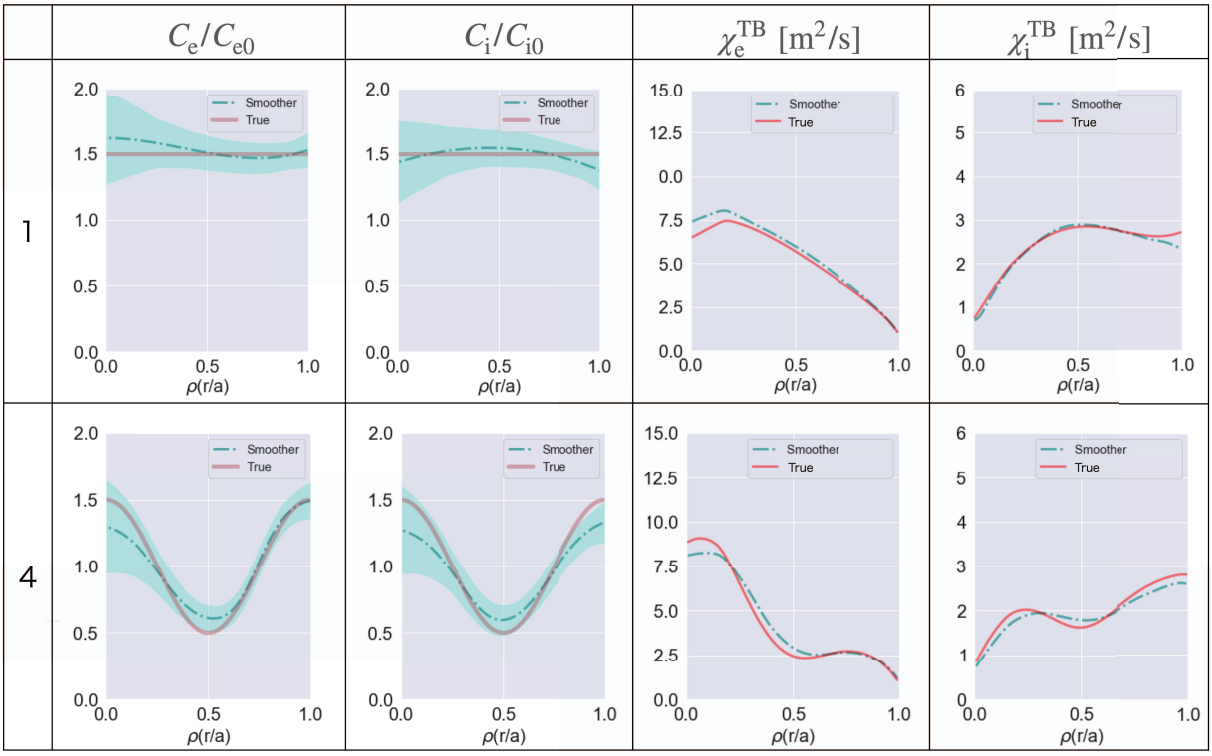

Fig. 4 Smoothed estimates of radial profile of C_e/C_{e0},C_i/C_{i0},χ_e^{TB} and χ_i^{TB} at time 1.0 s for Cases 1 and 4. The highlighted areas around the smoothed estimates represent the standard deviations of the smoothed ensemble.

around $C_s/C_{s0} = 1$. The EnKS corrects the estimates of the EnKF toward the average of the C_s/C_{s0} temporal change, $C_s/C_{s0} = 1$. This indicates that the EnKS follows the temporal trend of C_s in the time scale longer than the assimilation cycle. In Case 4, the smoothed estimates reproduce the true spatial variation of C_s/C_{s0} and stay around the true values. We have confirmed that the estimates of EnKS do not differ much form those of the EnKF for the same reason as Case 1.

Figure 3 shows the TASK3D simulation results of T_e and T_i using the smoothed estimates of C_s and k_s (dashed lines labeled 'TASK3D*') for Cases 1 to 4. In all cases, the results of both T_e and T_i agree reasonably with the observations. These results indicate the validity of the estimation by EnKS.

Figure 4 shows the smoothed estimates of the radial profiles of C_s/C_{s0} and χ_s^{TB} in Cases 1 and 4 at time 1.0 s. It is found that the smoothed estimates around the center ($\rho < 0.2$) have larger background errors than in the other region ($\rho > 0.2$). This indicates that the influence of C_s around the center region on the radial profiles of temperature in Eq. (1) is smaller than that of C_s in the other region because the temperature gradients around the center tend to zero. The errors between the true values and the smoothed estimates of C_i/C_{i0} around $\rho = 1$ in Cases 1 and 4 are also large. It is considered that the boundary condition in TASK3D affects the EnKF and EnKS estimate. Because the Dirichlet boundary condition is employed to solve Eq. (1) in TASK3D, the temperature around $\rho = 1$ is determined independently of χ_s. However, the estimates of C_s and χ_s^{TB} in $0.2 < \rho < 0.8$ agree well with the true values.

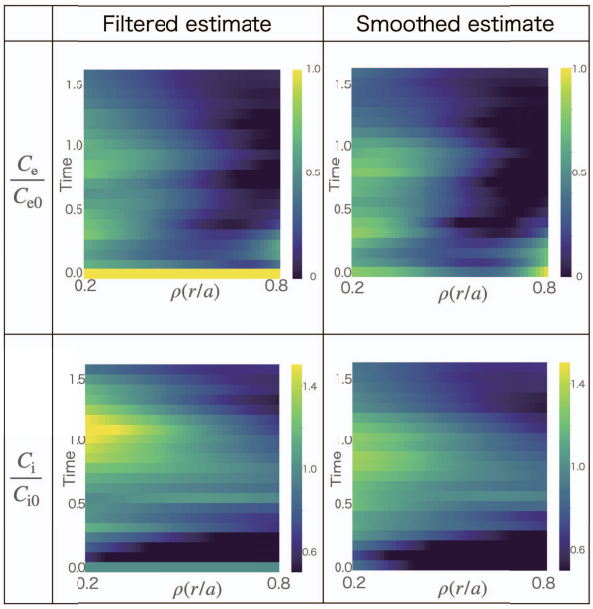

Fig. 5 Filtered and smoothed estimates of C_e/C_{e0} and C_i/C_{i0} in Case 5.

Figure 5 shows the filtered and smoothed estimates of C_s/C_{s0} in Case 5, and the temporal change of C_s/C_{s0} at $\rho = 0.25$ are plotted in Fig. 6. In Figs. 5 and 6, the es-

timates of C_e/C_{e0} and C_i/C_{i0} by EnKF are corrected and smoothed by the EnKS. In particular, the peak position of C_i/C_{i0} moves downward from 1.1 s in the filtered estimate to 0.9 s in the smoothed estimate in Fig. 5. This is the result of the EnKS correcting the filtered estimates

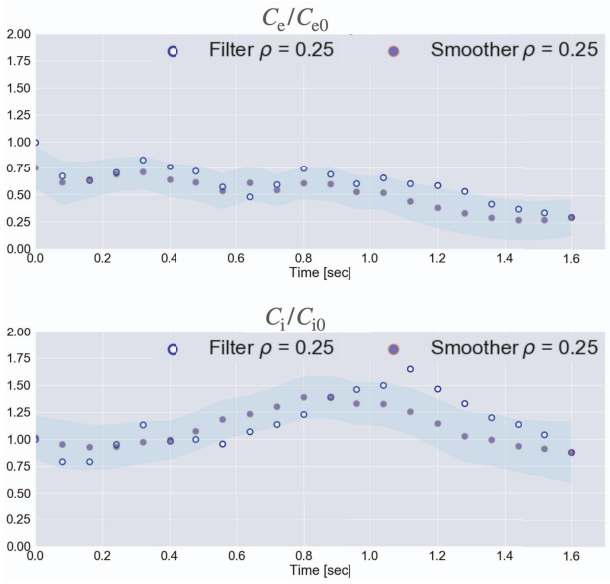

Fig. 6 Assimilation results of the temporal change of C_e/C_{e0} and C_i/C_{i0} at $\rho = 0.25$ in Cases 5. The highlighted areas around the smoothed estimates represent the standard deviations of the smoothed ensemble.

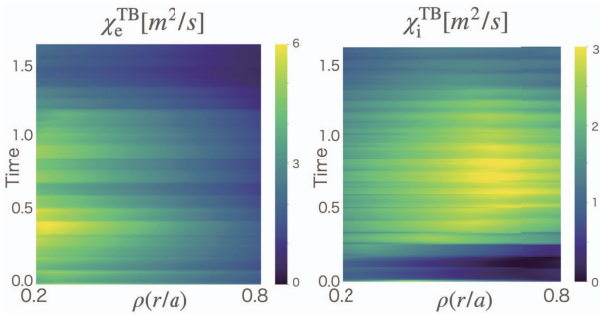

Fig. 7 χ_e and χ_i calculated using the smoothed estimates in Case 5.

to be reasonable both temporally and spatially using future data. Figure 7 shows the time-space distributions of χ_s calculated by using the smoothed estimates and Fig. 8 shows the TASK3D simulation results of T_e and T_i using the smoothed estimates of C_s and k_s in Case 5. In Fig. 8, we can confirm that the TASK3D simulation using the smoothed estimates can reproduce experimental temperature data with high accuracy.

The smoothed estimate of C_s includes information that should be considered in turbulent transport models to predict the temperature of plasma more accurately. If the smoothed estimates of C_s for various plasmas can be reproduced by a regression model, a more valid turbulent transport model can be obtained with relevant physical interpretation.

5. Summary

The EnKS has been introduced into ASTI to reasonably estimate the state vector both temporally and spatially. We have considered the uncertainties of temperature, density, the constant factor in the turbulent heat transport model, and the NBI heat deposition term. We have estimated the constant factors in the turbulent heat transport model, C_e and C_i, by assimilating the temperature and density profiles. The assimilation experiments for four simulated data-sets and the application to an experimental observation data-set in the LHD (shot number: 114053) have been performed.

It has been confirmed that the EnKS can estimate the radial profile of C_s with high accuracy for $0.2 < \rho < 0.8$ and that temporal trend of C_s, in a time scale longer than the assimilation cycle, from the assimilation of the simulated data-sets. Furthermore, χ_e^{TB} and χ_i^{TB} have been estimated for the experimental observation data-set, from the smoothed estimates of C_e and C_i, and the TASK3D simulation using the smoothed estimates has reproduced the experimental temperature data with high accuracy.

These results indicate the effectiveness and validity of the EnKS approach for accurate estimation of plasma parameters and the possibility of advanced turbulence modeling using the smoothed estimates of C_s for various plasmas.

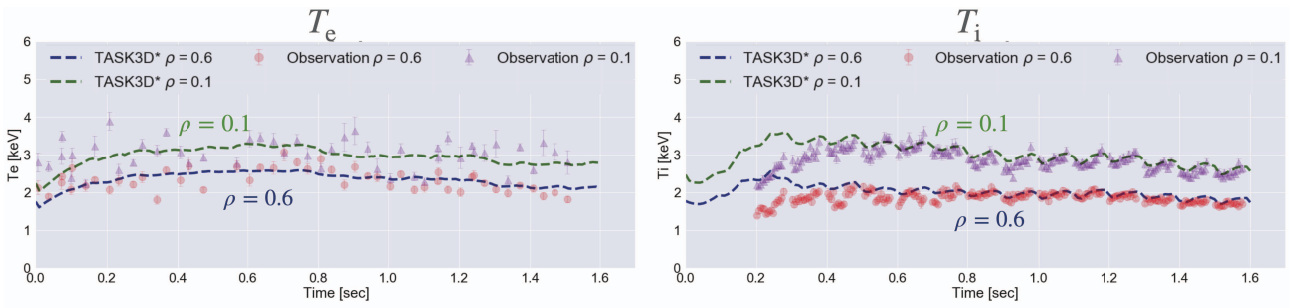

Fig. 8 TASK3D simulation results of T_e and T_i using the smoothed estimates of C_s and k_s for $\rho = 0.1$ and $\rho = 0.6$ in Case 5.

Acknowledgments

The authors acknowledge LHD Experiment Group for sharing the LHD experiment data which are essential for data assimilation. This work is performed on 'Plasma Simulator' (FUJITSU FX100) of NIFS. This work has been supported by the NIFS Collaborative Research Program (NIFS14KNTT025 and NIFS20KLPT007), ISM Cooperative Research Program (2019-ISMCRP-2027 and 2020-ISMCRP-2026), and collaborative research on the Remote Experiment Center (REC) of the International Fusion Energy Research Center (IFERC).

[1] Y. Morishita *et al.*, Nucl. Fusion **60**, 056001 (2020).
[2] G. Evensen, Ocean Dyn. **53**, 343 (2003).
[3] S. Murakami *et al.*, Plasma Phys. Control. Fusion **57**, 119601 (2015).
[4] G. Ueno *et al.*, SOLA **3**, 005-008 (2007).
[5] M.C.C. Messmer *et al.*, Plasma Phys. Control. Fusion **61**, 035011 (2019).
[6] A. Wakasa *et al.*, Proc. 39th EPS Conf. and 16th Int. Conf. Plasma Physics (Stockholm, Sweden, 2-6 July 2012) P2.028.
[7] H. Yamaguchi *et al.*, JPS Conf. Proc. **1**, 015045 (2014).
[8] A. Wakasa *et al.*, Contrib. Plasma Phys. **50**, 582-585 (2010).
[9] S.P. Hirshman and J.C. Whiston, Phys. Fluids **26**, 3553 (1983).
[10] H. Yamaguchi *et al.*, Plasma Fusion Res. **8**, 2403099 (2013).